Multiple Engineering Analyses in Exploring Cutting Marks of the Rip Saw

Weilong Chen
Department of Aeronautical Engineering, Chaoyang University of Technology, Taichung, Taiwan
Email: wchen@cyut.edu.tw

Fanglin Chao
Department of Industrial Design, Chaoyang University of Technology, Taichung, Taiwan
Email: flin@cyut.edu.tw

***Abstract*—The multiple saw's feeding system includes an auxiliary motor that drives the wheel and track in the workbench. Buffing wheels and chain pieces on the track provide stable holding of the log for structural stability. The mechanical factors cause cutting defects, which requires investigation of relative phenomena. Multiple engineering analyses enable quantitative mastering of related aspects to reach the solutions. The designer checked the chain's motion and adjusted the shape of the pieces to avoid the collision. The uneven shrinkage of casting samples improved after mold redesign. The chassis's deformation reduced through rib placed on the roller seat and frames. The modal analysis revealed the possible swing, which also affects the quality of the sawing. The frequency adjusting avoids the amplifying due to the excitation of motors. Changing the thickness of the chassis and increase the diagonal reinforcing bar could reduce the twisting amplitude. The case study confirms creatively utilized multiple engineering analyses with simplifying modeling skills benefits in system improvement.**

***Index Terms*—rip saw, spindle, engineering analysis, collision, thermal deformation, static analysis, modal analysis**

I. Introduction

A multi-piece rip saw system (Fig. 1) contains: groove spindle and multi-slice saw, pressuring feed system, photoelectric scanning system, and dust collection system. The "Groove spindle" is a cantilever beam with adjustable spacing that fixes the saw blade in a specific position and cut the wood with a rotary blade set. The main motor drives the saw blade attached to the spindle through the belt and controls the cutting range with a controller (Fig. 2).

A. Woodworking

The feeding system [1] is power by another motor to drive the "auxiliary power discharge wheel" (Fig. 3) and make the track run [2]. The crawler and chain pieces move the wood log undercut. The surface of these chains has a rough texture to enhance its friction. The downward pressing subjects the log by the press wheel that increases normal force and the friction with the bottom track to ensure stable moving in the right position [3] to saw by the blade.

B. FEM Modeling

The user found uneven scratches, which decline the quality of the wood cutting (Fig. 4). Researchers try to find out the possible problems and modify the processing setting to ensure the smoothness of the wood surface. CAE static structural analysis was used in calculating the structural deform by the external force. Static analysis can also judge whether the structure is strong enough and optimize structural materials.

Static analysis of diesel engine crankshaft utilized Pro/Engineer software [4] and ANSYS to identify the vibration modal and the deformation. The maximum strain appeared at the center of the crankshaft surface. The rigidity of the automotive chassis was analyzed to withstand the shock and vibrations. The chassis frame improved [5] by adding stiffener to reduce lateral bending.

The computational aspects of Galerkin's approximation were studied [6] using continuous piecewise polynomial basis functions. Limit and shakedown loads were obtained for a square plate with a hole and for a thin tube [7]. Rotating ring deformation showed the different precision of results with computation difficulty [8].

Figure 1. Multi-piece groove spindle.

Manuscript received September 8, 2020; accepted January 5, 2021.
Copyright credit, corresponding author Fanglin Chao

doi: 10.18178/ijmerr.10.2.72-78

Figure 2. Multi-piece rip saw machine (Kuang Yung Machinery)

Figure 3. An auxiliary power wheel

II. Materials and Methods

Woodcutting is an ancient technology; previously published papers in rip saw CAE simulation is lacking. In interviews with machine manufacturers, the researchers discovered the operating problems; and for the first time, and quantitatively confirmed by simulation. In this sequence research process, we have put forward four analysis results [9-12]. This paper will integrate various factors of the saw with an overall discussion.

When the multi-piece saw work, the high pressure and lateral tension apply the force to the log and the spindle. The spindle could be shortened or extended length due to tensile or compressive stress along the shaft's direction. The rod also affected the position of the saw blade and cutting quality. The external forces perpendicular to the shaft's direction may cause the spindle to bend and result in the cutting surface (Fig. 5).

A. Principle Parts of A Rip-Saw Machine

The Fig. 6 and 7 demonstrate principle parts of a rip-saw machine; were 1: upper cover (prevent wood chips from popping up), 2: dust collection pipeline, 3: saw shaft lifting motor (adjust roller seat height), 4: laser marking instrument, 5: feed guide plate (align with saw blades), 6: bulletproof tablets, 7: workbench, 8: crawler (conveying logs), 9: crawler brush, 10: control box, 11: vertical base (support fixed roller seat for up and down movement); 12/13: type A/B roller holder.

Increasing the cutting speed and avoiding possible quality problems is the main challenge in the design. This problem requires precise control of tool positioning to prevent defects on the wood surface caused by rapid cutting. The main parts related to cutting are connected and matched with each other. The relationship between those factors and components are organized in Fig. 6.

Figure 4. The curved skew line: pitfall mark on a log.

Figure 5. The internal chain, roller, and rip-saw of the woodworking machine (https://www.oavequipment.com)

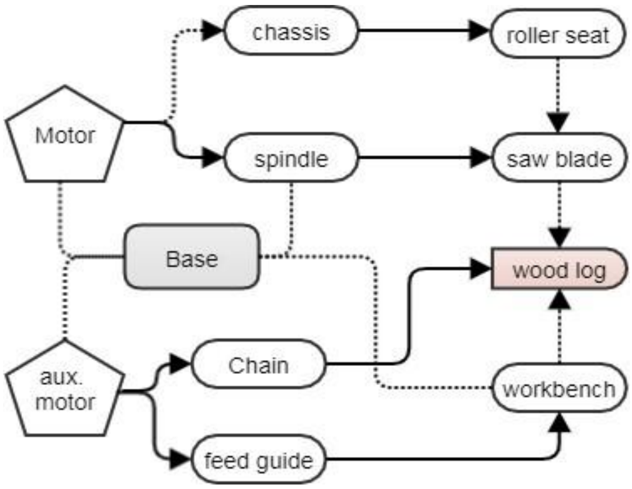

Figure 6. The relative functional components and their relation to the cutting marks.

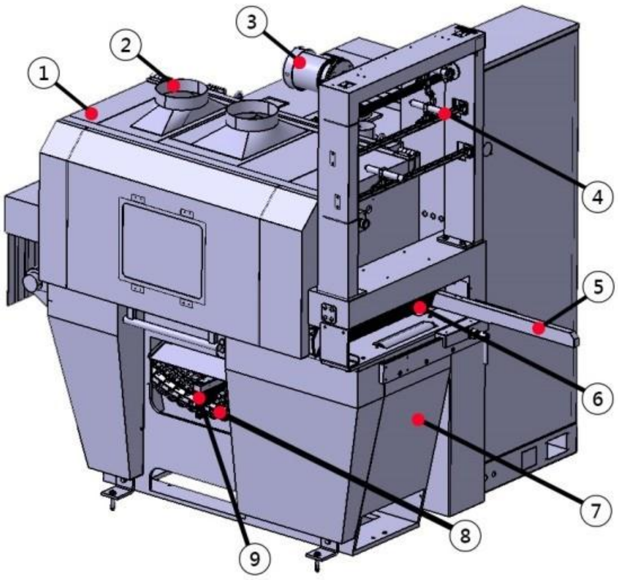

Figure 7. Principle parts and chassis of the machine

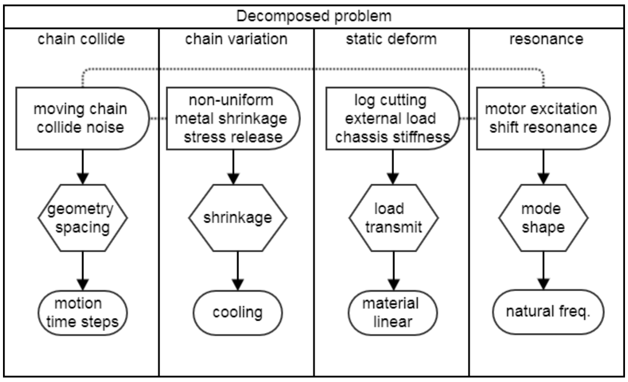

Figure 8. Related mechanical engineering principles of multiple engineering analysis

B. *The Related Engineering Principle*

The spindle material is steel, and the possible deformation by force can refer to the stress and strain curve diagram of the iron. When the strain is within the elastic limit, the stress is proportional to the pressure (Hook's Law). If the strain exceeded the limit, permanent plastic deformation would happen. A wide variety of stress-strain responses for stainless steel alloys were provided in [12]. This behavior is represented analytically by different material models in the analysis package.

The wood log is placed at the woodworking machine's feeding port and clamped by the roller and the crawler holder. Sufficient stiffness of the spindle is an essential consideration in the machine design. The lack of rigidity leads to axle deforming or irregular swing during operation and cutting quality.

Mechanical factors cause cutting defects, and the understanding of the principle requires the help of engineering analysis. The comprehensive engineering principles sorted out the design-related factors from complex problems. Because these physical phenomena are related to each other, and the components' connections are complicated, the researchers grouped them into four main categories (Fig. 8). In this problem decomposing way, the critical parameters can be identified in different engineering analysis methods.

III. Results: Collision of a Fast Moving Chain

A chain piece is a symmetrical structure with two v-shaped grooves in contact with the track—a raised curved block-shaft placed on each recess. The chain piece is subjected to the y-direction force and transmitted to the track through the v-shaped groove.

A. *Dynamic Modeling*

The chain moves along the x-direction driven by the motor. The normal force generates adequate friction to avoid log instability during cutting. SimDesigner rigid body motion analysis utilized to observe detail movement and relative force status. The Crash workbench enabled to evaluate the degree of adherence to the requirements of the mechanisms. We assumed the track is fixed, and the chain piece is simple supported by the v-rails. A simplified section model of the track guide was built using five connected chains (Fig. 9) with ball bearings [13]. The rigid body motion analysis shows chain hits a lower guide and simultaneously hitting the other track. This collision causes the rear-side of the front-end top up the rear piece's front side and will be pushed up.

B. *Collision Prevention*

The excitation force is the pulling force (150 N, 5-sec step function) to keep the log moved on track. The original model had a 136 mm track pitch. Results of a motion simulation (Fig. 10) revealed the rear-end of the chain was topped up with a short track pitch, and the front-end of the follower piece was lifted. This unstable situation caused the log shift; parameter adjustment can minimize the chain's topped. When the guide groove gap decreased (upper and lower clearances were 0.2 and 0.3 mm) and the distance between the entrance and exit of the track increased to 6 mm, which minimized the chance of collision.

When the chain's guide angle was adequately controlled, the chain piece's stability and the quality of the feed system improved. The impact amplitude (maximum N value) of the redesign chain piece also reduced from 1298.4 to 613.5; when the distance is 8 mm, the collision significantly reduced.

IV. Results: Chassis Structural Static Analysis

The original chassis deformed when the spindle and the press wheel were loaded; deformation data helped us find the right auxiliary structure needed. The analysis focuses on the variation of static load and total deformation of the spindle. The stress and strain results reveal the structure's reinforced possibility.

Due to the steel spindle's rigidity and a limited amount of external force, we assumed that the component is within the linear region. This linear hypothesis was validated after the strain was calculated. The boundary conditions between components are set to (1) The axis and the bearing holes are close contact during rotation regardless of the tolerance; (2) Specifying the distance between the components with contact parameters.

A. Roller Seat

A multi-piece saw contains many subsystems, and each system included many components; strategies are needed to simplify the FEM model. Simplified geometries were employed in non-stressful areas — secondary components such as motors replaced with a lumped mass. The 3D geometric represented with a 2D extruded curve; we also removed the rounded corners and holes. In static analysis, two types of roller seats (A/B) were compared to deduced deformation. Fig. 11 shows a simplified model of type-A and B roller seat. The parameters or boundary conditions need to verify iteratively before simulation. After the simplified model passed the validation, the engineer proposed the new structure to achieve the design goal.

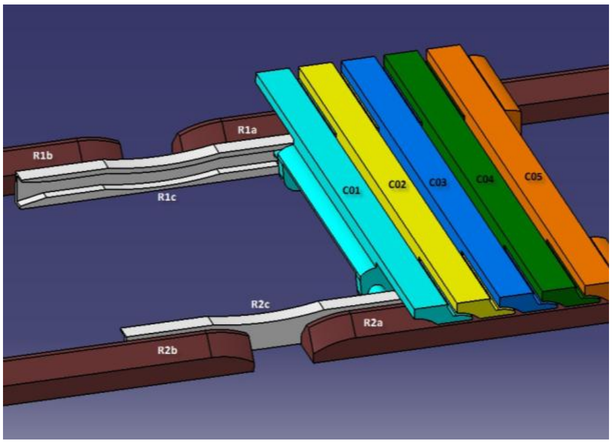

Figure 9. SimDesigner simplified model for rigid body collision analysis. The track is denoted by R1a, R1b, R2a, and R2b; R1c and R2c denote the guide slot; c-01 denotes the five chain pieces to c-05.

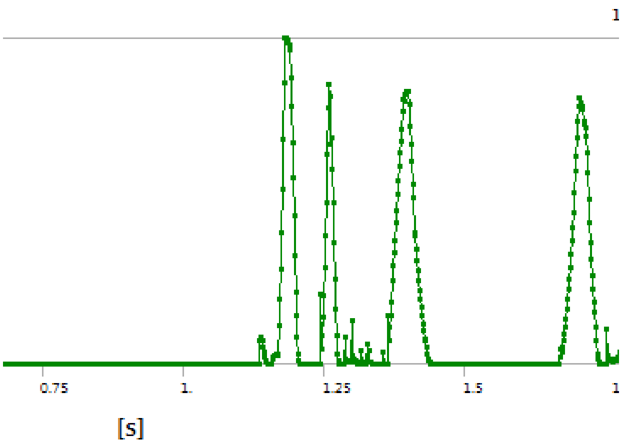

Figure 10. Rigid body impact force on c-02: Adding the guide groove (upper and lower clearances were 0.2 and 0.8 mm, respectively), the impact amplitude at the c-02 changed to be 1019 N.

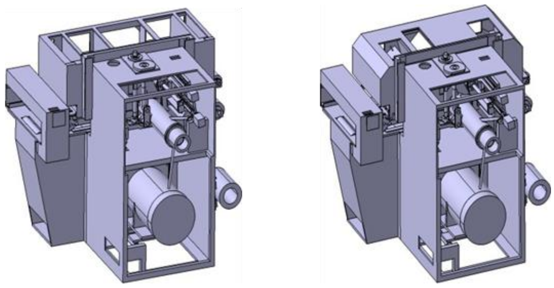

Figure 11. Type-A/B roller seat after simplification (3D geometric are simplified into 2D geometric shapes)

The Advanced Size function set to on: curvature, in “Relevance center” set to “Coarse," minimum mesh size: 2mm, maximum mesh size: 18mm. In the typical areas, the mesh size is crude for reducing the computation time. The number of mesh and computation is reduced by simplifying modeling to observe the amount of deformation at the roller seat.

The spindle and saw system employed an auxiliary feed and press system to guide the logs along the sawing area in a stabilized way. The logs are subjected to transverse and longitudinal external forces; the press wheel needs a particular mesh discretization to reflect the wood transmission direction. The boundary and load conditions are:

1) The contact point continues to change during the rotation;
2) Depending on the reaction force, we give each roller seat 1000N to the lower force and provided 4000N to hold the log (Fig. 12);
3) The external force decomposed into +y direction and -x-direction's (represents the strength of the downward pressure and the cutting) reaction force to facilitate the analysis.

B. Roller Seat Deformation

The roller seats hold the roller, which is in contact with the wood log. There are chain pieces supported by track rail. Both roller seat and track hold the wood under processing. Therefore, the deformation of these parts under external force is critical. The roller seat and track deformation by external force were analyzed. With a total of eight pips of roller seat and workbench track, displacement data help us to understand "whether the quality of cutting produces offset?" The static analysis results show in Fig. 13, which allows a structural selection for subsequent improvements.

When the roller receives the force in the +Y direction, the roller seat will be deformed in the +Y direction, causing the roller not to clamp the log. If the saw is widened, it will affect the picking rate of the wood. When the roller receives a force in the -X direction, the roller seat is deformed in the -X direction, causing the roller position to shift. If the wheel offset affects the direction of the feeding, it may also cause sawing marks.

Fig. 14 shows the detailed structure of the rollers seat. The deformation of the roller seat is much larger than the track. The track segment is placed on the work surface with strong support; the roller seat relies on the upper pressing force. The stress and deformation analysis results are significantly different from B and A, especially at position 12, where type-B reduced significantly. The opening of the roller seat A is relatively large, which affects the rigidity of the structure. B's opening space is reduced, the intermediate frame structure is integrated, and the structural strength is increased. Therefore, the B roller seat can clamp the log and withstand the force in both the +Y direction and the -X direction.

C. *Spindle Deform*

The two roller holders' structural strength was observed by applying a force of 1000 N in the forward direction. Fig. 12 shows the spindle deformation and stress distribution (+Y direction). As shown in Fig. 15, the main shaft subjected to the - X direction force, the maximum stress is 25.07 Mpa, and the maximum deformation is 0.36 mm (B-type is smaller).

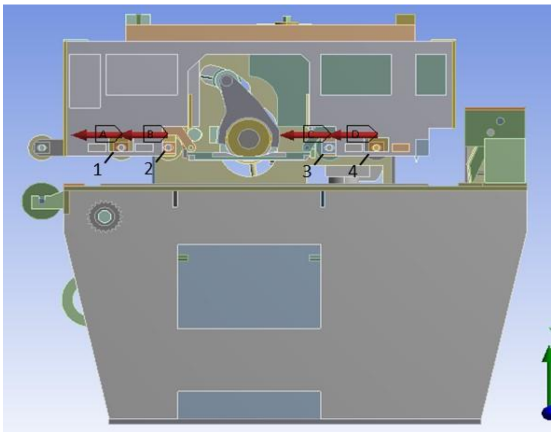

Figure 12. The roller shaft is subjected to the -X direction force placed on location A,B,C,D, and the displacement calculations of roller seats are placed on location 1,2,3,4.

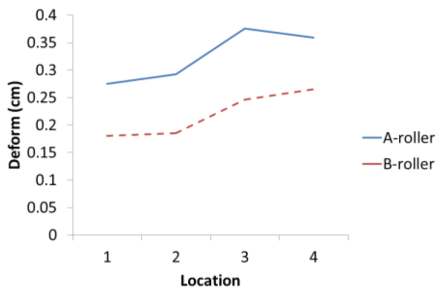

Figure 13. The roller seat applied a -X direction force, the displacement in the Y direction

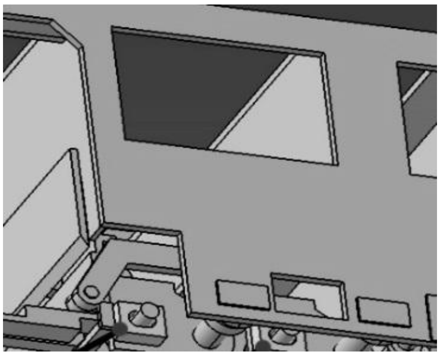

(a)

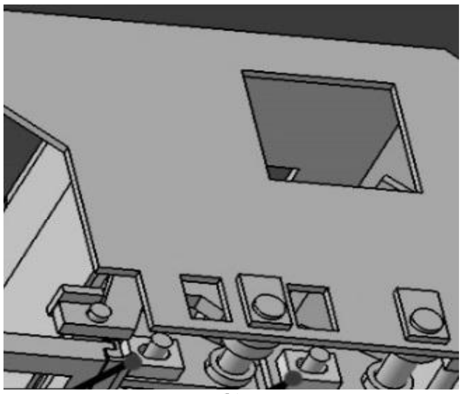

(b)

Figure 14. Detail structure of roller seat (the A-B type).

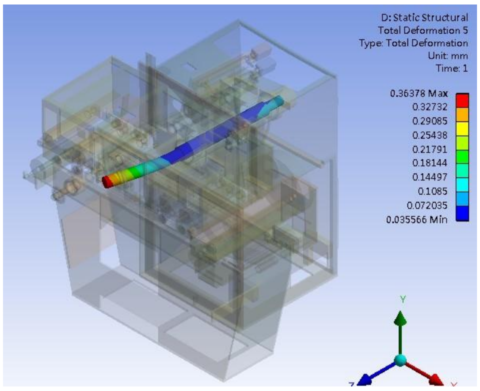

Figure 15. The deformation and stress distribution of the spindle are 0.36mm and 25M

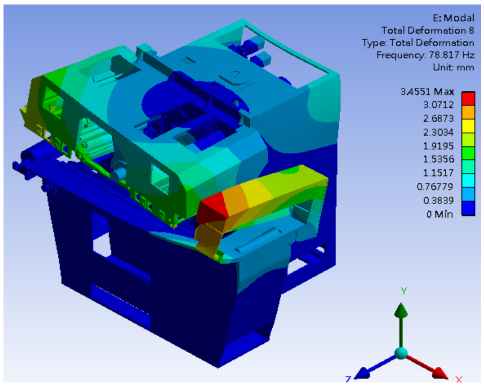

(a)

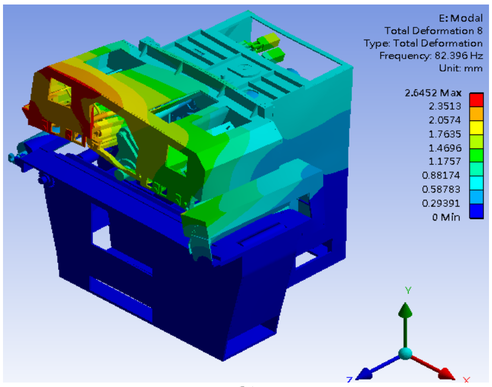

(b)

Figure 16. The mode-8 is resonant at the roller seat, in which the stand is twisted. The original machine (a) is 78.8Hz, and the modified design (b) is 82.3Hz [14]

V. Results: Modal Analysis Results

Modal parameters are solved with boundary conditions of simplified geometry. We add structural parts on the chassis to shift the natural frequency to prevent amplification. Modal adjusting confirms the benefits of improved design. The mode-4 is excited by a motor that pulls the spindle to resonate the stand. The original frequency was 67.3Hz and modified to 60.2Hz. The shape of mode-5 revealed the stress concentrated on the feed rack and the bottom of the table; the original frequency was 72.3Hz and modified to 74.4Hz, stress focused on the stand, and the bracket that suspends the servo motor [14,15]. The mode-8 is the resonance twisted at the roller seat; the horizontal rib limited the vertical bend and rotated (Fig. 16). The original frequency was 78.8Hz and modified design is 82.3Hz. When deviating from the harmonic frequency of the motor, the chance of resonance decreases.

Observe the difference between the adjusted machine mode shape and the original one; we confirmed the modified design's benefits. The widened L-shape truss extended structural strength. By changing the rib placement and frame stiffness, the deformation keeps within an acceptable range. According to the analysis results, reinforcing ribs added on the roller seat successfully avoids amplifying and reduce the twisting.

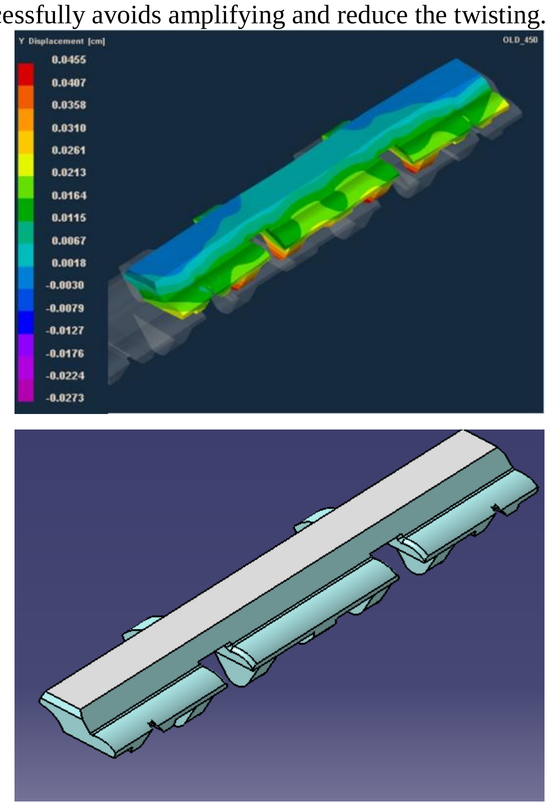

Figure 17. Chain piece made by sand casting, the Y displacement (cm) happens during the solidification process.

VI. Results: Thermal Deformation after Molding

The chain pieces require a flatness surface to stably supporting the log. The molten metal is injected into a hollow mold made of a high-temperature resistant material and solidified [16] to accomplish the desired shape. Chain pieces sometimes deformed after demolding. The metal gradually solidifies inward from the surface and shrinkage due to thermal stress release [17]. Fig. 17 shows the non-uniform surface of a bent chain, the Y displacement (cm) happens during the solidification process. The researcher use ProCAST casting process analysis to simulate the stress presented during the solidification [18]. Fig. 17 also indicated the areas with substantial stress changes or stress concentrations are likely to be deformed. Proportional shrinkage approach is utilized to reduce the warpage problem.

Based on the calculated stress distribution, a rib structure was added to the chain block to enhance the overall flatness. The rib was placed on the mold's bottom surface and filled in the gaps appearing on edges. The updated chain body did not twist after being cooled. The formed chain piece demonstrated a proportional shrinkage during the crystallization, and the thermal displacement is under control. The chain samples demonstrated a reasonable flatness on the working plane. This mode of block improvement reduces the need for secondary processing.

VII. Discussion of Results

The novelty of work is mainly sorting out the factors related to the cut marks in the sawing process, including conditions that directly affect the saw blade or are indirectly changed by the motor. The causes are divided into four types of phenomenon. They are static load, structural resonance, uneven chain, and collisions during fast movement. We defined the degree of influence through four engineering analyses, respectively, optimize the product structure from the four factors. Adding structural reinforcement ribs or reducing the chance of resonance and avoiding the casting mold flow cooling process's shrinkage show its effectiveness.

The four physical phenomena are separated and affect each other. After we implemented each improvement and optimization, the overall machine operation speed has accelerated. The modified machine's vibration noise is low, and the wavy cutting marks on the workpiece's surface are reduced. By improving overall operational efficiency, we have validated the improvement through analysis of the above four phenomena.

Future implications of current work make the research more applicable. Many parts in a complex mechanical structure affected and coupled with different operating conditions. The engineer can analyze those phenomena with existing software. Although there is a coupling effect between phenomena, separate analysis, and improvement parameters can reduce problems. In the face of complex machine operations, designers first establish a digital model and then use numerical simulation to understand the problem factors and influence intensity in the overall operation to achieve optimization.

VIII. Conclusion

The sawing speed is essential to increase the production rate —buffing wheels and chain pieces on tracks provided log holding. The pulling force and holding pressure on chain pieces caused deformation and create noticeable cutting marks. By changing the rib placement on a roller seat, the engineer reduced the maximum spindle deformation. The stress concentrated on the roller seat's core caused the roller seat to swing and affect the sawing quality. Limited the vertical bend by extra ribs placement on the roller seat can change mode shape. Mode-8 was 78.8Hz and the resonance twisted at the roller seat; after modification, this frequency shifted to 82.3Hz with less twisting.

A buffing wheel and track hold the log, but the moving chain pieces also generate shaking. Kinetic simulation help engineer predicts possible collision. By changing the spacing and adding guide rails, the amplitude of collision impact was reduced significantly.

The shrinkage of chain pieces minimized through adjustment of the mold block cavity. Modified casting samples were reasonably flat on their working plane. The improved design reduces material consumption and processing costs. The multiple engineering analyses explored related phenomena with cutting marks to help an engineer meet the machine specifications with less cutting defects.

Conflict of Interest

The authors declare no conflict of interest.

Author Contributions

W. L. Chen conducted the research project and CAE simulation; F. L. Chao analyzed the data and wrote the paper; all authors had approved the final version.

Acknowledgment

The authors wish to thank Y.H Lin and C.C. Chang for CAD modeling. The study was supported partially by Kuang Yung Machinery Co. Ltd.

References

[1] T. W. Hahn, "Automated multiple rip saw feeding apparatus," U.S. Patent No. 4,945,797. 7 Aug. 1990..

[2] L. R. Livick and L. Lester, "Adjustable device for feeding workpieces of different thicknesses past a rip saw for cutting purposes," *U.S. Patent*, 4,026,173, 1997.

[3] E. Kline, J. K. Wiedenbeck, and P. A. Araman, "Management of wood products manufacturing using simulation/animation," *Forest Products Journal*, vol. 42, no. 2, pp. 45–52, 1992.

[4] MSC-Simdesigner. [Online]. Available: http://www.mscsoftware.com/assets/ sim designer-catia_edition_ds.pdf.

[5] J. P. Roop, "Computational aspects of FEM approximation of fractional advection-dispersion equations on bounded domains in R2," *Journal of Computational and Applied Mathematics*, vol. 193, no. 1, pp. 243–268, 2006.

[6] P. N. Bogdanovich, D. A. Bliznets, A. O. Shimanovsky, and V. I. Yakubovich, "Theoretical and experimental analyses of the sawing process for hard and ultra-hard materials," *International Journal of Mechanical Engineering and Robotics Research*, vol. 7, no. 2, 2018.

[7] J. Mart ńez, J. Dumas, S. Lefebvre, and L. Y. Wei, "Structure and appearance optimization for controllable shape design," *ACM Transactions on Graphics*, vol. 34, no. 6, pp. 1–11, 2015.

[8] F. Star ý, "Different approaches to calculation of rotating ring deformations of wrapping machine," *Modern Methods of Construction Design*, Cham: Springer, 2014.

[9] Y. Wang, B. Sun, Q. Wang, Y. Zhu, and W. Ding, "An understanding of the hot tearing mechanism in AZ91 magnesium alloy," *Materials Letters*, vol. 53, no. 1-2, pp. 35–39, 2002.

[10] A. G. Goryunov, O. V. Egorova, K. A. Kozin, S. N. Liventsov, N. V. Liventsova, and O. V. Shmidt, "Optimization and diagnostics code for technological processes: Radiochemical production simulator," *Atomic Energy*, vol. 124, no. 5, pp. 321–325, 2018.

[11] Y. L. Hwang, J. K. Cheng, and V. T. Truong, "Computer-aided dynamic analysis and simulation of multibody manufacturing systems," *Applied Mechanics and Materials*, vol. 764-765, pp. 757–761, 2015.

[12] M. Heitzer and M. Staat, "FEM-computation of load carrying capacity of highly loaded passive components by direct methods," *Nuclear Engineering and Design*, vol. 193, no. 3, pp. 349–358, 1999.

[13] W. L. Chen and F. L. Chao, "Track design of woodworking rip-saw chain," *International Journal of Mechanical Engineering and Robotics Research*, vol. 8, no.5, 2019.

[14] W. L. Chen and F. L. Chao, "Structural resonance analysis of multi-piece rip saw," in *Proc.73th Forest product convention*, July 2019, Atlanta USA.

[15] W. L. Chen and F. L. Chao, "Finite element resonance analysis of the complex structure of a crosscut saw machine," *Forest Products Journal*, vol. 70, no.1, 2020.

[16] J. O. Kristiansson, "Thermal stresses in the early stage of solidification of steel," *Journal of Thermal Stresses*, vol. 5, no. 3-4, pp. 315–330, 1982.

[17] Arrayago, E. Real, and L. Gardner, "Description of stress–strain curves for stainless steel alloys," *Materials & Design*, vol. 87, pp. 540–552, 2015.

[18] W. L. Chen and F. L. Chao, "CAE supported improvement of chain casting of ripsaw for woodworking," *International Journal of Materials, Mechanics and Manufacturing*, vol. 7, no. 4, pp. 185–189, 2019.

Weilong Chen received the Ph.D. degree in Aerospace engineering from University of Oklahoma. He was a researcher of MSC software, he also served as consultant in several company such as Pro-Iroda, Grand Mate and aerospace institute.
He joined National Center for High-Performance Computing, Hsinchu, Taiwan. Since September 1999, he has been an Associate Professor with the Department of Industrial Design at Chaoyang University of Technology, Taichung, Taiwan. He joined Department of Aeronautical Engineering in 2019. His research interests include CAE, and product development.

Fanglin Chao received the Ph.D. degree in electrical engineering from National Taiwan University. He joined the Electronic Research and Service Organization, Industrial Technology Research Institute, Hsinchu, Taiwan, in 1982. In 1994, he was an Associate Professor with Da-Yeh Institute of Technology. Since September 2004, he has been an Associate Professor with the Department of Industrial Design at Chaoyang University of Technology, Taichung, Taiwan. His research interests include eco-design, and design integration in product development.